80-711

объединенный
институт
ядерных
исследований

дубна

928/1-81

E1-80-711

A.P.Cheplakov, D.K.Kopylova,
A.I.Shklovskaya, Yu.A.Troyan

STUDY OF INELASTIC d + C_3H_8 INTERACTIONS AT P_d = 4.6, 8.2 AND 10 GeV/c ACCOMPANIED BY THE EMISSION OF SECONDARY DEUTERON WITH MOMENTUM LARGER THAN $P_d/2$

1980

SELECTION OF INELASTIC INTERACTIONS
WITH SECONDARY FAST DEUTERON

Inelastic $d + C_3H_8 \rightarrow d' + \ldots$ interactions* with fast secondary deuteron have been studied using a 2m propane bubble chamber (High Energy Laboratory, JINR) at $P_d = 4.6$, 8.2 and 10 GeV/c.

The pictures obtained were scanned for events of all multiplicities with positive particles emitted at any angle and having momentum $P_d/2$. The track length, ℓ, of these particles was larger than ℓ_{lim} which provided a relative error of $\leq 15\%$ in measuring momentum (fig.1). The one-step scanning efficiency of such events for all P_d was (85-90)%. After the tracks of fast particles (fast particles are referred to as those with $P > P_d/2$) had been measured on semiautomatic devices and calculated using the geometric program 1-6 [1], their momentum spectra were constructed (fig.2). In the figure one can observe a stripping part of the spectrum at each P_d, where the fast particle is a proton. Next are the region of inelastic $d + C_3H_8 \rightarrow d' + \ldots$ interactions, where deuterons are mainly produced (the superstripping region denoted by the dotted line), and the region of elastic interactions. The mean relative error in measuring fast particle momenta was (7-9)%.

The free path of positive particles from the superstripping region has been determined in paper [2]. Of these particles the fraction of deuterons is equal to $(100 \, {}^{+\,0}_{-\,20})\%$.

The number of cumulative protons in the superstripping region was estimated at $P_d = 4.6$ GeV/c. We used
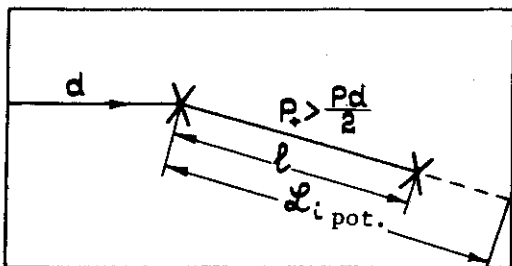

Fig.1. Schematic view of the events selected.

___

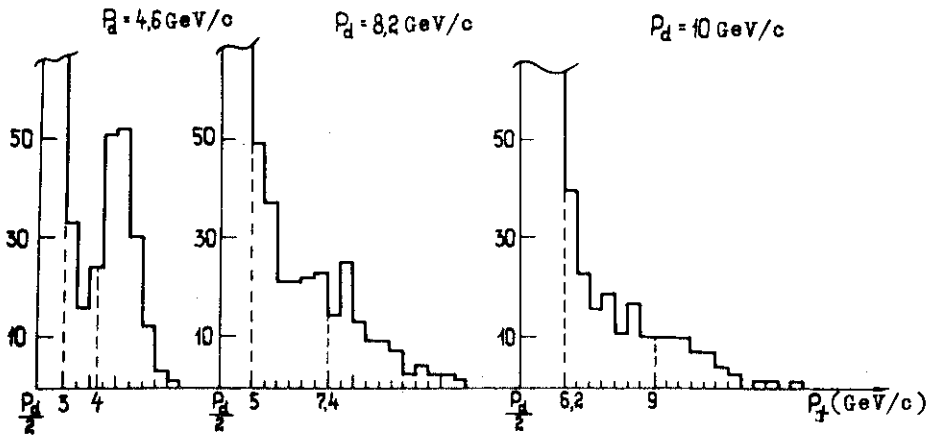* d′ is used to denote secondary deuteron in distinction to primary one.

1

Fig.2. Momentum distributions of fast positive particles at different P_d with a step of 0.4 GeV/c. In the figure is presented only the high-energy part of the stripping spectrum. The dotted lines and figures on the momenta axis are limits between the momentum regions.

the data of paper [3] devoted to studies of cumulative proton production in dp interactions at $P_d = 3.33$ GeV/c using chamber technique. If one assumes that the production cross sections of cumulative protons coincide at $P_d = 3.33$ and 4.6 GeV/c, their fraction among the particles in the super-stripping region is 17%. In electronics experiments [4,5], where dC interactions were investigated at $P_d = 3.5$ and 6.3 GeV/c and positive particles were detected in superstripping momen-tum regions at angles of 2.5° and 6°, respectively, the frac-tion of protons was <10%.

Boundary momentum values between stripping and superstripp-ing regions at different P_d were chosen so that the contami-nation of stripping protons in the particles from the super-stripping momentum region did not exceed 10%. Data on measuring errors of the stripping protons, taking their length into ac-count, were obtained from the distributions of primary protons at $P_d = 4.1$ and 5 GeV/c. The momentum spread of protons due to Fermi-motion inside deuterons was small [7]. The chosen boun-dary values were somewhat larger than $T = 0.02$ GeV (T is the kinetic energy of secondary protons in the d rest system) cor-responding to the transitional value of T from stripping to cumulative protons [3,7]. Thus, at the chosen boundary momentum

2

values the contamination of stripping protons was 6% at $P_d =$
$= 4.6$ GeV/c, 6% at $P_d = 8.2$ GeV/c and 4% at $P_d = 10$ GeV/c.

The boundaries between the regions of inelastic and elastic
interactions are values of $P_{d'}$ in reactions $dp \rightarrow d'p\pi$
with one π-meson production at corresponding P_d.

After choosing the boundaries of superstripping regions, all
events having fast particle in this momentum region were comp-
letely treated.

Inelastic interactions in a propane chamber look as one-
and two-prong events. One can observe two-prong events only
in the case when the recoil proton has a momentum of >160 MeV.
According to the kinematics of elastic dp events, this cor-
responds to a fast deuteron emission angle of $\geq 2.5°$ for $P_d =$
$= 4.6$ GeV/c, $\geq 1.5°$ for $P_d = 8.2$ GeV/c and $\geq 1.3°$ for $P_d = 10$ GeV/c.
The larger P_d the larger the number of one-prong events has
a small emission angle of fast particle, and, consequently,
the larger losses of elastic events (see. fig.2). Using the
relations obtained from the kinematics of elastic dp events,
the elastic interactions observed in the superstripping re-
gion due to measurement errors were selected and rejected.
After this cleaning, in inelastic interactions there remained
the class of nonidentified events the contamination of which
was $<10\%$. As will be seen later on, the admixture of elastic
events estimated by analysing the effective dp mass distribu-
tion (fig.5a) at $P_d = 8.2$ and 10 GeV/c is $\sim 8\%$.

Thus, in the chosen superstripping momenta region there
are mainly secondary deuterons produced in $d + C_3H_8$ inelastic
interactions. The contamination of stripping and cumulative
protons is from 10 to 20%, and that of deuterons from elastic
events is $<10\%$.

Figure 3 presents the momentum distributions of negative and
positive particles produced in inelastic interactions. These
distributions do not contain the fast deuteron. Positive par-
ticles are denoted by the solid histogram; negative ones, by
the dotted line.

A possible identification of positive particles has been
made. To identify slow particles, momentum-range and momentum-
ionization relations were used. The particles from the region
of momenta from $(0.7-0.8)$ GeV/c to $P_{max}(\pi^-) = P_{lim}$ remained
nonidentified, and the particles having $P_+ > P_{lim}$ were
classified as protons (P_{lim} are shown in fig.3 by arrows).

PROPERTIES OF INELASTIC INTERACTIONS WITH FAST DEUTERON
AS A FUNCTION OF P_d

Table 1 presents some characteristics of inelastic interac-
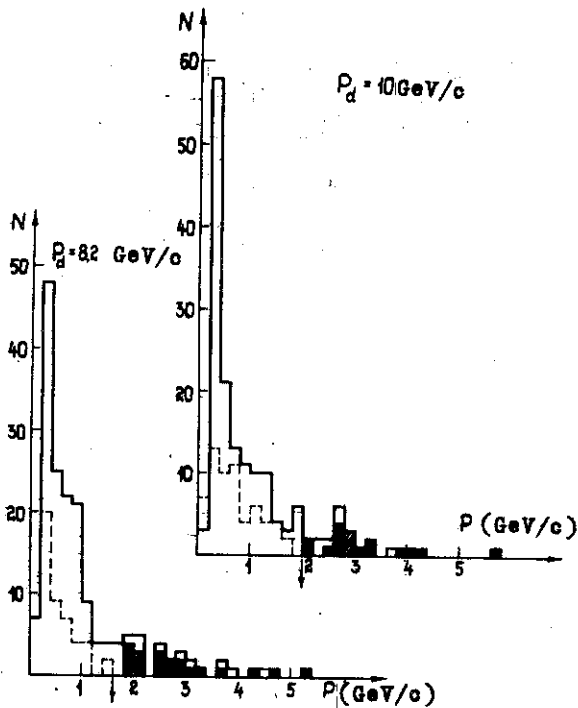tions with fast proton as a function of P_d and of the type

3

Fig.3. Momentum distributions of secondary positive (solid histograms) and negative (dotted line) particles. The values of P_{lim} are denoted by arrows. The dashed area is the momentum distribution of particles 2.

of events. The number of interactions under study at each P_d is shown in the first column of the table. The events were divided into dp and dC using the conventional criteria applied in a propane chamber /9/. Deuteron interactions on free protons (dp') and on quasi-free protons (dp$_C$) were classified as dp events. The remaining events were attributed to the type of dC interactions. One-prong events and, in part, interactions with nonidentified particles were classified as (dp-dC) events.

As is seen from the table, secondary deuterons fly out at small angles with respect to the direction of the primary track, and average space angle $\theta_{d'd}$ decreases with increasing P_d. The average multiplicity of charged particles and the number of π^- —mesons per interaction increase with increasing P_d more in dC than in dp interactions. Within errors, the average transverse momenta of secondary deuterons are independent of P_d and of associative event multiplicity and coincide with the average transverse momentum of π^- —mesons at $P_d = 8.2$ and 10 GeV/c. Within errors, the average value of momentum transfer from primary to secondary deuteron does not depend on P_d and is equal to (0.58 ± 0.02) (GeV/c)^2. The table presents the cross sections of inelastic processes with secondary deuteron emission in the superstripping regions. These cross sections rise with increasing P_d. However, the cross sections should be de-

4

Table 1

$\bar{P}$ GeV/c (number of events)	Type of interaction	$\bar{N}_{ch}$	$\bar{N}_{\pi^-}$	$\bar{\theta}_{dd'}$	$\bar{P}_\perp(d')$	$\bar{P}_\perp(\pi^-)$	$\overline{\Sigma P_\parallel} \pm \overline{\Delta\Sigma P_\parallel}$	σ mb $d+C_3H_8 \rightarrow d'+\ldots$
4,6 (57)	dp	2,16±0,II	0,08±0.05	5°30	0,32±0,03	0,24±0,03	3,7I±0,29	24±4 (3,0-4,0) GeV/c
	dC	3,I0±0,I9	0,39±0,I0					
	Σ	2,35±0,I3	0,I2±0,03					
8,2 (I74)	φp	2,50±0,09	0,23±0,05	2°50	0,28±0,02	0,26±0,03	6,80±0,59	55±5 (5,0-7,4) GeV/c
	dC	4,3I±0,2I	0,54±0,09					
	Σ	2,87±0,II	0,32±0,04					
I0 (144)	φp	2,34±0,09	0,I7±0,04	2°20	0,30±0,02	0,3I±0,03	8,32±0,70	85±7 (6,2-9) GeV/c
	dC	3,98±0,I8	0,82±0,09					
	Σ	2,97±0,II	0,47±0,05					

5

Table 2

P per nucleon	$\bar{N}_{ch}$		
	$d+(C_3H_8)\rightarrow d'+...$	$d+(C_3H_8)$ /9/	$\dfrac{[p+(C_3H_8)]+[n+(C_3H_8)]}{2}$
2.3 GeV/c	2.35+0.13	3.2+0.06	2.38+0.07
4.1 GeV/c	2.87+0.11	3.81+0.08	2.70+0.11

P per nucleon	$\bar{N}_{\pi^-}$ interaction		
	$d+(C_3H_8)\rightarrow d'+...$	$d+(C_3H_8)$ /9/	$\dfrac{[p+(C_3H_8)]+[n+(C_3H_8)]}{2}$
2.3 GeV/c	0.12+0.03	0.34+0.09	0.23+0.03
4.1 GeV/c	0.32+0.04	0.51+0.02	0.38+0.03

creased by (10-20)% keeping in mind the above-mentioned con-
tamination of protons. To determine the cross sections, cor-
rections are introduced taking into account the loss of events
with fast track length <ℓ_{lim} (fig.1) and the scanning effi-
ciency. The errors presented are statistical.

The differential cross sections of deuteron production in
the superstripping momenta region have been measured in dp
and dC interactions at an angle of 6° for P_d=4.3 and 8.9 GeV/c/5/.
Using our data, it has been found that the cross section de-
creases by a factor of ~1.3 with increasing P_d from 4.6 to
8.9 GeV/c at (5-7)° which agrees with pape /5/.

For comparison with our data, Table 2 gives the average
multiplicities of charged particles and the number of π^--me-
sons per interaction for all deuteron-propane and nucleon-
propane collisions at the same momenta of primary particles
per nucleon.

ENHANCEMENT OF THE d'p EFFECTIVE MASS DISTRIBUTION

The effective mass distribution of d'p combinations at dif-
ferent P_d was plotted for inelastic interactions with fast
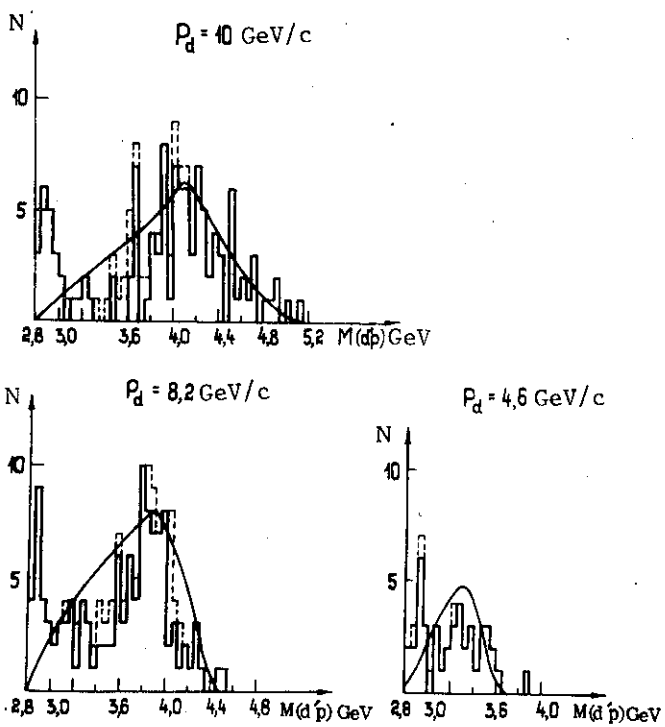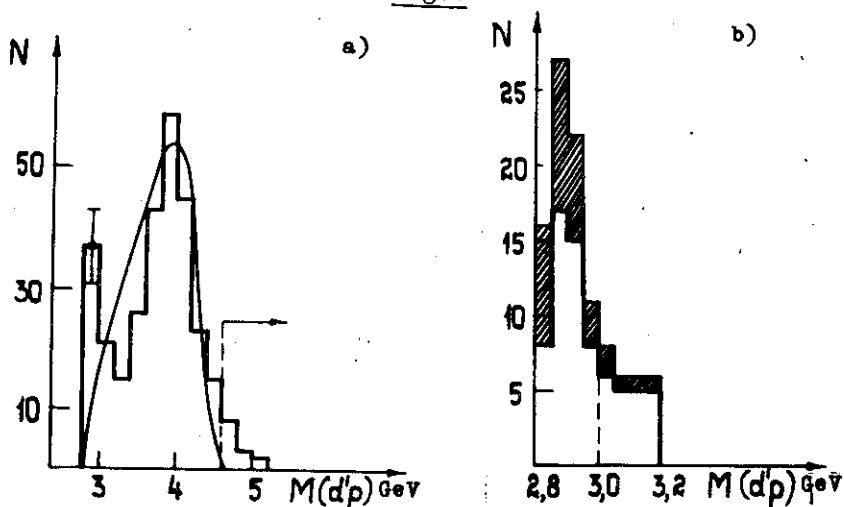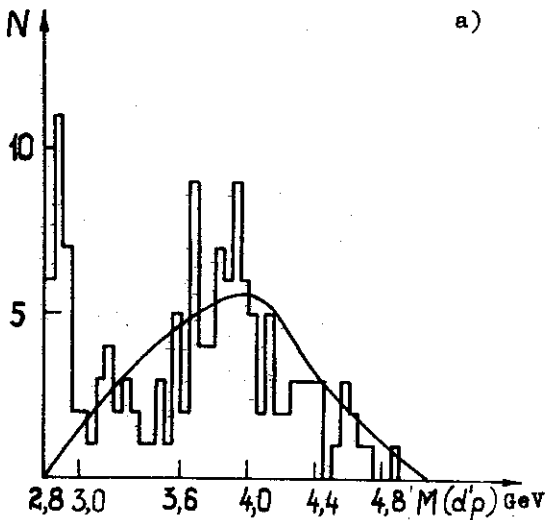deuteron production (fig.4). In addition to identified protons,

Fig.4

Fig.5. Effective mass d′p distributions at different P_d (the figures are described in the text).

the distribution contained protons of the group of nonidentified π^+/p particles treated as follows: assuming that all positive particles in the event, except the deuteron, were protons, the $M(d'p)$ distribution was plotted, and the $M(d'p)$ distribution plotted for $d'\pi^-$ combinations was subtracted from it when the proton mass was assigned to the π^--meson. If one assumes that the momentum and angular distributions of π^--and π^+-mesons coincide, the difference of the above distributions gives the $M(d'p)$ distribution for real protons. The effective mass spectrum was compared to the background distribution from phase space. Reactions $dN \to d'N(k\pi)$, $k=1,2,3$ were generated, whereupon the events having secondary deuteron momentum within the same limits as in the experiment were selected, and the $d'N$ effective mass was plotted for them.

The experimental histograms are best described if the background curve contains 90% events of the $dN \to d'N\pi$ reaction and 10% events of the $dN \to d'N2\pi$ reaction. (The solid curves in all figures are normalized to the total number of combinations in the experimental histograms). One can observe a good agreement of the background curves with the experimental distributions at all P_d on the right side of the effective mass spectrum. The mass value corresponding to the distribution maximum increases with increasing P_d in this part of the spectrum. In an effective mass range of (2.8-3) GeV at all P_d one can observe a peak which is not described by the background generated for dN interactions. In fig.5a is plotted the summary $M(d'p)$ distribution with a step of 0.2 GeV from the events produced by deuterons having $P_d = 8.2$ and 10 GeV/c. A statistical error is indicated in the region $M(d'p) = (2.8-2)$ GeV. The background curve is drawn in the above manner. Figure 5b presents the summary $M(d'p)$ distribution with a step of 0.05 GeV only in the region of effective masses (2.8-3) GeV for $P_d = 4.6$, 8.2 and 10 GeV/c. The average mass value in the distribution peak is equal to 2.90 GeV (which is ~70 MeV larger than the sum of the d and p masses), and the total peak width is ~100 MeV.

The type of events having $d'p$ effective mass within (2.8-3) GeV has been studied. The peak in this region of effective masses is generated by two fast particles. As we have determined previously, one of them is a deuteron (identified as 1) and another is a positive particle having momentum equal, on average, to 0.5 P_d' (it is designated as particle 2 ,see fig.6b). The momentum distribution of particles 2, identified as protons, is presented in fig.3 (the dashed part of the distribution). Knowing that the peak in the effective mass spectrum in a range of (2.8-3) GeV is generated by two fast par-
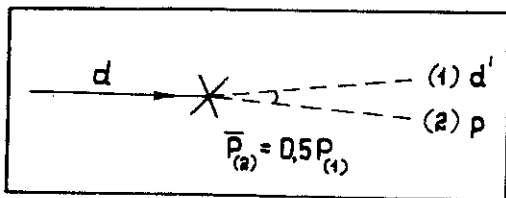
a)

b)

$$\bar{P}_{(2)} = 0.5 P_{(1)}$$

Fig.6. a) Effective mass distribution of deuterons with identified protons in dC events for P_d=8.2 and 10 GeV/c. The background curve is plotted for dN interactions. b) Schematic view of the events having the d'p effective mass at (2.8-3) GeV.

ticles 1 and 2, an additional selection of similar events has been made at P_d = 8.2 GeV/c. The effective mass distribution of particles 1 and 2 in these regions is shown in fig.5b (dashed part). The distributions presented previously do not contain these events.

It has been found that the interactions having $M_{ef}(d'p) = (2.8-3)$ GeV contain dn_C (32%), dC' (36%) and dp (32%) events. Since in the carbon nucleus the number of interactions on quasi-free protons and neutrons should be equal, all dp events of the peak are interactions on quasi-free protons. Consequently, all interactions having $M(d'p) \approx (2.8-3)$GeV occur on the carbon nucleus. Figure 6a presents the $M(\overline{d'p})$ distribution for P_d = 8.2 and 10 GeV/c only for dC events(dn_C+dC'). Most dC interactions (80%) are similar to those occurring on free nucleons as $M_{ef}(d'p)$ from these events is well described by the background generated for dN interactions. The remaining dC interactions having $M(d'p) =$ =(2.8-3) GeV (~20%) occur so that the nucleus wave function should be taken into account for their explanation.

In order to prove that correct masses are assigned to particles 1 and 2, their additional identification has been made. To determine a possible contamination of π^+–mesons in the group of particles 2, the momentum distributions of π–mesons were considered in the $dN \to d'N 2\pi$ reaction at $P_d = 8.2$ and 10 GeV/c generated as described above (fig.7a). The reaction with the production of precisely two π–mesons was chosen since particle 2 assumed to be a π–meson was added to the π–meson already available in the interaction. One can see from the distribution that the production of π–mesons having $P_\pi > P_{lim}$ is kinematically allowed in the $dN \to d'N 2\pi$ reaction. Assuming that these π–mesons (π–mesons having $P > P_{lim}$) are protons, the dp effective mass spectrum is plotted (fig.7b). As is seen from the figure, in the region of effective masses (2.8-3) GeV there are only 10% of all d′p combinations. The spread of the π–meson spectrum due to the interaction on quasi-free nucleons (mean Fermi-momentum is taken to be 0.25 GeV/c) results in increasing the contamination of π–mesons by a factor of 1.5. Thus, the contamination of π^+–mesons in the group of particles 2 is no more than 15% both for $P_d = 8.2$ GeV/c and for $P_d = 10$ GeV/c.
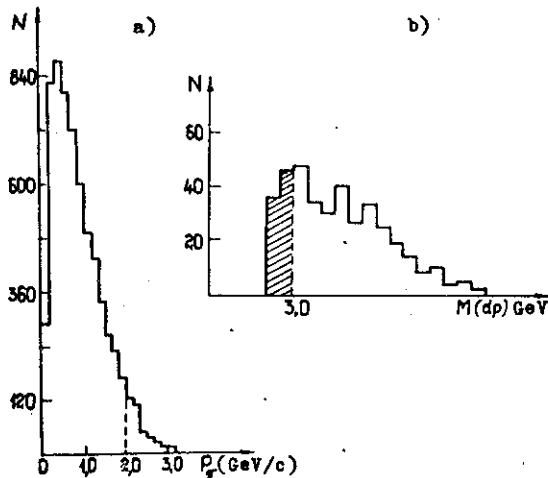

Fig.7. a) Distribution of π–mesons in the $dN \to d'N2\pi$, reaction at $P_d = 10$ GeV/c generated by phase space with further selection by secondary deuteron momentum, b) d′p effective mass spectrum assuming that π–mesons having $P_\pi > 2$ GeV/c are protons.
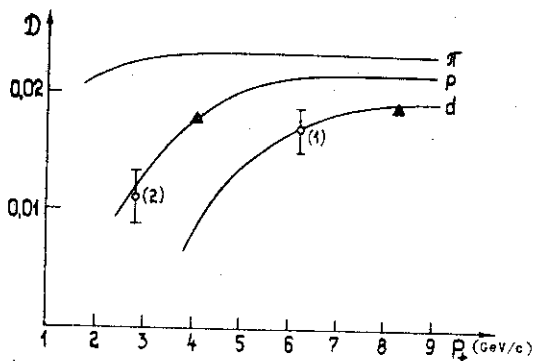
Fig.8. Densities of δ -electrons D (cm^{-1}) as a function of π -meson, proton and deuteron momenta in propane.

The next method of particles identification is their statistical mass classification versus the density of δ -electrons (D) having $E^{\delta} > E^{\delta}_{min}$ on the particle tracks. The theoretical curves (fig.8) are graduated with respect to the density of δ -electrons having $E^{\delta} \geq 1$ MeV on the tracks of beam deuterons for $P_d = 8.2$ GeV/c and of beam protons for $P_d = 3.8$ GeV/c (points ▲). Using the same criteria, the density of δ-electrons was measured on the tracks of particles 1 and 2 continued to the second part of the 2m propane bubble chamber. The values of D obtained for the tracks of particles 1 and 2 are given in fig.7 together with its statistical errors. The chosen value of D corresponds to the average momentum value over the whole group of particles 1 or 2.

According to the formulae $R = \dfrac{N' - N_{exp}}{N' - N''}$ and $\Delta R = \dfrac{\sqrt{N_{exp}}}{N' - N''}$ presented in paper /10/, the fraction of deuterons, R_d, was determined in the group of particles 1 (N' and N'' are the values of D for protons and deuterons, respectively) and the fraction of protons, R_p, in the group of particles 2 (N' and N'' are the values of D for π-mesons and protons). It was found that $R_d = 1 \pm {}^{0}_{0.4}$ and $R_p = 0.90 \pm 0.15$.

Further the method was used to find free paths in the groups of particles 1 and 2 which also made it possible to estimate the particle composition in these groups /2/. On the tracks of particles 1 and 2 continued to the second part of the chamber, secondary interactions were selected. Knowing average potential length L and the number of secondary interactions in the groups of particles 1 and 2, we determined the fraction of deuterons, a_d, in the group of particles 1 and the fraction of protons, a_p, in the group of particles 2. In this case we used known free paths for deuterons ($L_d = 80$ cm), protons
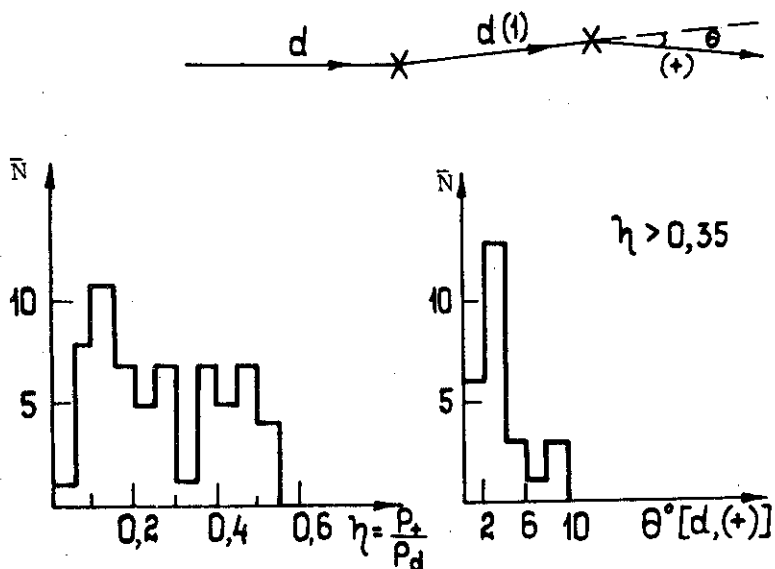
Fig.9. Momentum and angular distributions of fast positive particles produced in the interactions of particles 1 with propane and schematic view of these interactions.

($L_p = 125$ cm) and π-mesons ($L_\pi = 165$ cm) in propane[2,11]. Due to insufficient statistics, we obtained the values of α with large errors: $\alpha_d = 0.78 + 0.30$ and $\alpha_p = 0.60 + 0.46$.

An attempt was made to identify particles 1 by momentum and angular distributions of secondary positive particles produced by particles 1 (fig.9). In the momentum spectrum of secondary particles some number of tracks having $\eta > 0.35$ was observed which are likely to be stripping protons from deuteron disintegration. Their angular distribution is similar to that of stripping particles. However, due to insufficient statistics for secondary interactions, it is difficult to draw a conclusion of the number of deuterons in the group of particles 1. Despite the fact that each afore-described method of statistical particle identification by mass gives a large error, they all taken together support the following conclusion drawn previously: group 1 particles are deuterons and group 2 particles are protons.

Table 3

Events having $M_{eff}(d'p) = (2.8-3)$ GeV

P_d GeV/c	$\overline{N}_{ch}$	$\overline{N}_{\pi^-}$	$\overline{\Sigma P_{\parallel}} \pm \overline{\Delta \Sigma P_{\parallel}}$	$\overline{\theta}_{d'p}$	$M(d'p)$	σ (mb)
4.6 (10)	3.01+0.3	0.41+0.09	4.58+0.34	20°	2.91	2+1
8.2 (20)	3.80+0.19	0.65+0.10	9.02+0.65	9.5°	2.88	5+1.5
10 (17)	3.35+0.22	0.71+0.13	10.90+0.87	7°	2.90	8+2.5

Decreasing the contamination of protons in the group of particles 1 can be achieved by increasing limiting momenta between the stripping and superstripping regions. However, such a procedure decreases the number of events in the peak thus decreasing the total number of inelastic events to the same degree. The previous limiting momenta were left but an additional error (~15%) was introduced to the cross sections due to the some uncertainty in identification (Table 3). Table 3 presents the characteristics of the events having effective mass $M(d'p)$ in a range of (2.8-3) GeV as a function of P_d. From the table one can see that despite large errors, the production cross section of such events is likely to rise with increasing P_d and is (1-2)% of the inelastic dC cross section. Within the errors, the average effective mass corresponding to the distribution peak is independent of P_d ($\Delta M = 25$ MeV). The space angle between the deuteron and the proton decreases with increasing P_d (see Table 3).

Figure 10 presents the distribution of the sums of the longitudinal momenta for charged particles in each event ($\Sigma P_{\parallel}$) at different P_d (the dashed events have $M(d'p) = (2.8-3)$ GeV). Unlike all interactions (Table 1), the average values of $\Sigma P_{\parallel}$ in the events having $M(d'p) = (2.8-3)$ GeV at $P_d = 8.2$ and 10 GeV/c (Table 3) exceed the corresponding primary deuteron momenta, P_d, by more than one error. The error in measuring $\Sigma P_{\parallel}$ was calculated as $\sqrt{\Sigma \Delta P_i^2}$. In order to clarify whether errors in particle momenta lead to the excess obtained experimentally, some estimates were made. Knowing the error, $\overline{\Delta \Sigma P_{\parallel}}$, and using
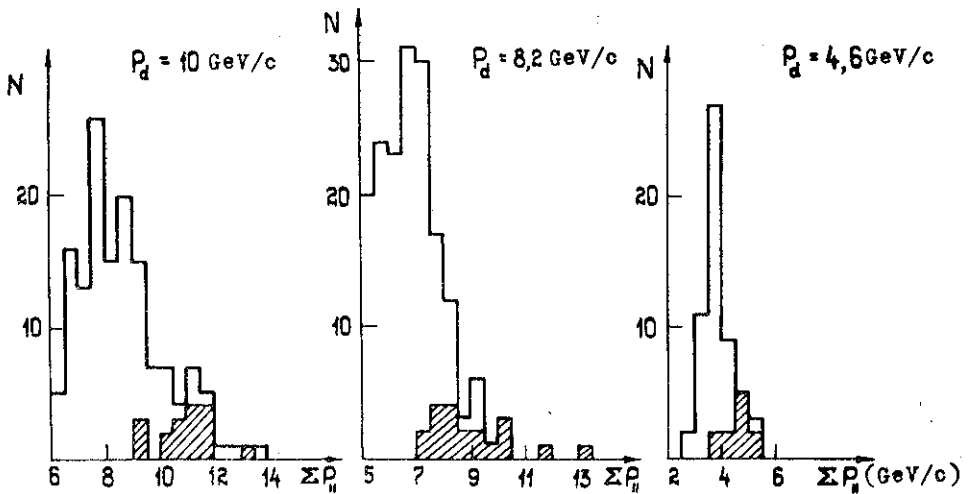
13

Fig.10. Distribution of the sums of the longitudinal momenta for charged particles in the events at different P_d.

the probability integral, the number of events was determined having $\Sigma P_\parallel$ larger than the chosen value of P' due to the measurement errors. The difference of the observed number of interactions having $\Sigma P_\parallel > P'$ from that explained by the measurement errors is within a two-fold error ($\Delta = 7 \pm 4$ for $P_d = 8.2$ GeV/c and $\Lambda = 10+5$ for $P_d = 10$ GeV/c).

The available statistics does not allow one to draw a conclusion of the presence of physics effect.

CONCLUSION

The $d + C_3H_8 \rightarrow d' + \ldots$ interactions at $P_d = 4.6$, 8.2 and 10 GeV/c with fast deuteron production represent collisions with momentum transfer from the primary to the secondary deuteron independent of P_d and having an average value of $0.58+0.02(GeV/c)^2$. Within the errors, the multiplicity of charged particles in these events coincide with that of all $N + C_3H_8$ interactions having the same primary particle momentum per nucleon (<u>Table 2</u>). The peak having an average mass of 2.90 GeV and a width of ~ 100 MeV is observed in the effective mass distributions of dp combinations for all P_d.

Despite large errors, the obtained production cross sections of the events in the peak region are likely to show evidence for their rise with increasing P_d.

14

The events with fast secondary deuteron having $M(d'p) = (2.8-3)$GeV are nucleus-nucleus interactions. One can observe $(1-2)\%$ such interactions of all inelastic dC events. They are not described by the background generated for deuteron interactions on free nucleons. To study the nature of the effect observed, statistics should be increased.

REFERENCES

1. Markova N.F. et al. JINR, P10-3768, Dubna, 1968.
2. Abdivaliev A. et al. JINR, 1-11590, Dubna, 1978.
3. Aladashvili B.S. et al. Ya.F., 1978, vol.27,3, p.704.
4. Papp J. LBL-3633, 1975.
5. Azhgirej L.S. et al. Ya.F., 1978, vol.27, 4, p.1027; Ya.F., 1979, v.30, 6(12), p.1578.
6. Gasparian A.P. et al. JINR, 1-9111, Dubna, 1975.
7. Abdivaliev A. et al. JINR, 1-9924, Dubna, 1976.
8. Abdurakhimov A.U. et al. JINR, P1-6277, Dubna, 1972; JINR, P1-6326, Dubna, 1972.
9. Angelov N. et al. (Collaboration). Ya.F., 1979, vol.30,6, p.1590.
10. Bem Ya. et al. JINR, P-2842, Dubna, 1966.
11. Akhababian N. et al. JINR, 1-12114, Dubna, 1979; Barashenkov V.S., Toneev V.D. Interactions of High-Energy Particles and Atomic Nuclei with Nuclei. Atomizdat, Moscow, 1972.